

Development of Recycling Technology for High-Impurity Spent Refractories into High-Alumina Castable

KUN-MING CHEN*, CHIA-HUNG KUO*, TUNG-HSIN SU*,
CHUN-JUNG HUANG** and CHEN-SHIUN CHOU**

**New Materials Research & Development Department*

***Steelmaking Department
China Steel Corporation*

Spent bricks from torpedo cars were primarily recycled for use in iron-runner refractories and tap-hole clay, which utilized only the high-purity and coarse-grained fractions. However, up to 20-30% of the spent refractory material consisted of high-impurity powder with excessive levels of Fe_2O_3 and CaO , which could not be effectively recycled. This study investigated the effects of adding high-impurity powder to high-alumina castable (CA-17) at addition levels of 2.5%, 5%, 7.5%, and 10% by weight. The results showed that increasing the addition of spent refractories caused a slight increase in water demand and a significant reduction in permanent linear change (PLC). Compressive strength exhibited a slight improvement, while both porosity and bulk density experienced minor deterioration. These trends were attributed to the formation of low-melting phases due to the reactions between the impurities and the base CA-17 components (Al_2O_3 and SiO_2). Additionally, slag resistance, steel penetration resistance, and refractoriness declined with higher addition rates. Nevertheless, performance remained acceptable up to a 5% addition, beyond which notable degradation occurred. Based on an annual CA-17 usage of 900 tons at China Steel Corporation, the approach enabled the recycling of approximately 45 tons of high-impurity spent refractories per year. This contribution to resource recovery and sustainable material management was achieved through the technology developed in this study.

Keywords: Spent refractories, Recycling, High-alumina castable

1. INTRODUCTION

In recent years, the rapid advancement of clean steel production technology has made secondary ladle refining a critical stage in the steelmaking process. However, as steel grades diversify and tapping temperatures increase, the operational conditions for ladles have become increasingly severe. The high-alumina castable CA-17 is primarily applied to the ladle mouth area during relining operations. In addition, CA-17 is widely used in other areas within China Steel Corporation (CSC), including the surfaces of ladle transfer car rails, the spout zone of iron ladles, and around the nozzle-seat bricks in the tundish. CA-17 is mainly composed of alumina (Al_2O_3). The coarse aggregate primarily consists of diaspore, and its size distribution is optimized according to the Andreasen model⁽¹⁾. The powder matrix comprises alumina powder, calcium aluminate cement (CAC), silica (SiO_2), clay, and various additives⁽²⁻⁵⁾. At China Steel Corporation, CA-17 has been developed into a mature product meeting industrial requirements.

China Steel Corporation has actively developed

recycling technologies for spent refractories with a primary focus on recovering spent refractory bricks from torpedo cars. The recycling process involves crushing, screening, and magnetic separation. The yield of crushed coarse aggregate with relatively high purity is approximately 70-80%, which is mainly applied in iron-runner refractories and tap-hole clay. However, up to 20-30% of the spent refractories consists of high-impurity powder with excessive levels of Fe_2O_3 and CaO , which cannot be effectively recycled. This study investigates the effects of adding high-impurity powder to high-alumina castable CA-17 to achieve effective recycling of spent refractories.

2. EXPERIMENTAL METHOD

The composition of high-alumina castable CA-17 for steel ladles is divided into three types, including aggregates (particle size >200 mesh), powders (particle size ≤ 200 mesh), and additives. This study consisted of diaspore ($\text{Al}_2\text{O}_3 \geq 85\%$, $\text{SiO}_2 \leq 15\%$), with different particle sizes: 5-8 mm, 3-5 mm, 1-3 mm, and 0.075-1 mm. Powders included alumina ($\alpha\text{-Al}_2\text{O}_3 \geq 99\%$, $D_{50} \leq 5\mu\text{m}$)

and silica ($\text{SiO}_2 \geq 97\%$, $\text{D}_{50} \leq 1 \mu\text{m}$). In terms of additives, calcium aluminate cement ($\text{Al}_2\text{O}_3 \geq 70 \text{ wt}\%$, $\text{CaO} \leq 30 \text{ wt}\%$) was adopted as the primary binder due to its high refractoriness and rapid setting behavior, while sodium hexametaphosphate was introduced as a dispersant to improve slurry flowability.

The objective of this study was to incorporate varying proportions of spent refractories into high-alumina castable CA-17, with the bricks from torpedo car selected as the source of the spent refractories. The recycling process of spent bricks involved crushing, screening, and magnetic separation. The yield of crushed coarse aggregate with relatively high purity is approximately 70–80%, which is mainly applied in iron-runner refractories and tap-hole clay. However, up to 20–30% of the spent refractories consisted of high-impurity powder with excessive levels of Fe_2O_3 and CaO , which cannot be effectively recycled. The chemical composition of the processed spent bricks from the torpedo car is presented in Table 1.

This study examines the effects of adding 0%, 2.5%, 5%, 7.5%, and 10% high-impurity spent refractory powders to CA-17. Samples were labeled CA-(1) to CA-(5). The aim was to identify the optimal addition level and compare it with the current material to promote resource reutilization.

In terms of sample preparation, the high-alumina castables were first prepared with aggregates, powders, and additives in the designed proportions. An appropriate amount of water was added to the mixer, mixed for 3 minutes, poured into molds, and left to stand for 24 hours. After demolding, the samples were dried in an oven at $110^\circ\text{C}/24\text{hrs}$, and then sintered at $1500^\circ\text{C}/3\text{hr}$ for property analysis.

The analysis items included the following:

- (1) The standard test method for measuring consistency of self-flowing castable refractories (ASTM C1446-19).
- (2) For bulk density (BD) and apparent porosity (AP)

were measured using a density tester (Precondar, XQK-04)

- (3) Permanent linear change (PLC) measurement according to JIS R2208 for
- (4) The modulus of rupture (MOR) test was conducted using a Hung-Ta, HT-2402 universal testing machine in accordance with ASTM C583-15.
- (5) Cold crushing strength (CCS) at room temperature was measured by ASTM C133-97.
- (6) The steel block penetration test was conducted using medium carbon steel at $1600^\circ\text{C}/15\text{min}$ in accordance with (JIS R2214).
- (7) Microstructural analysis was performed using a polarizing microscope and a scanning electron microscope (SEM) equipped with energy-dispersive spectroscopy (EDS).

3. RESULTS AND DISCUSSION

3.1 Effect of Adding Spent Refractories on Workability and Physical Properties

The workability and fundamental physical properties of high-alumina castable CA-17 with varying additions of spent refractories are presented in Tables 2 and 3, respectively. Regarding workability, the experimental results showed that as the addition level of spent refractories increased, the required water content slightly increased while the flowability remained largely unaffected. In terms of physical properties, a higher addition level of spent refractories led to a significant decrease in the permanent linear change (PLC), a slight improvement in mechanical strength (MOR and CCS), and a marginal decrease in both apparent porosity (AP) and bulk density (BD). These changes in physical behavior were primarily attributed to the elevated levels of contaminants such as CaO and Fe_2O_3 in the spent refractories, which reacted with the components of the CA-17 to form low-melting phases that promoted sintering. The addition of spent refractories, therefore, tended to deteriorate the workability and physical properties of CA-17.

Table 1 Chemical composition analysis of torpedo car spent bricks with different particle sizes .

Spent bricks of torpedo car	Particle size (mm)				
	Element (%)	8-5	5-3	3-1	1-0.075 Powder
$\text{CaO} (\leq 1)$		0.383	0.512	0.427	0.475 1.754
$\text{Al}_2\text{O}_3 (\geq 65)$		71.7	81.7	79.8	73.9 38.99
$\text{Fe}_2\text{O}_3 (\leq 1.5)$		1.26	1.32	1.34	1.18 3.73
H_2O		0.179	0.111	0.178	0.264 0.751
Production ratio (%)		4.80	14.4	28.7	21.5 30.6

*Powder: <200 mesh (< 0.075mm)

Table 2 Effects of spent refractory addition on water demand and flowability of CA-17.

Sample		Water demand	Flowability
Addition of spent refractories (wt%)		(wt%)	(%)
CA-(1)	0	10	15
CA-(2)	2.5	10	11
CA-(3)	5	10.5	12
CA-(4)	7.5	10.5	15
CA-(5)	10	11	18

Table 3 Effects of spent refractory addition on the physical properties of CA-17.

Addition of spent refractories		Physical properties and specification (@1400°C /3H)				
		PLC	MOR	CCS	AP	BD
		-1.5~+0.5 %	≥ 7.5MPa	≥ 19 MPa	≤ 30%	≥ 2.15 g/cm ³
CA-(1)	0 wt%	0.03	12.4	46.7	27.9	2.55
CA-(2)	2.5 wt%	-0.37	15.1	58.6	27.7	2.52
CA-(3)	5 wt%	-0.49	13.8	57.1	27.1	2.52
CA-(4)	7.5 wt%	-0.62	15.5	62.7	26.7	2.52
CA-(5)	10 wt%	-0.97	16.1	63.6	26.2	2.51

3.2 Effect of Adding Spent Refractories on Steel Penetration Resistance, Slag Corrosion Resistance, and Refractoriness

The steel penetration resistance of CA-17 samples containing varying amounts of spent refractory fine powders is summarized in Table 4. Cup-shaped specimens were prepared and filled with medium-carbon steel, then heated to 1500°C and held for 3 hours. The maximum penetration depth of molten steel at the specimen base was measured, and the sample surfaces were inspected for cracks or steel leakage. The results showed that samples with spent refractory additions ranging from 2.5% to 10% exhibited no steel leakage and only minor surface cracking. However, increasing the proportion of spent refractories led to a greater maximum steel penetration depth, which indicated a reduction in resistance to molten steel penetration. The slag corrosion resistance of samples containing spent refractory additions is shown in Table 5. The test involved placing slag inside the specimens and heating them to 1650°C for 30 minutes, after which the used slag was removed and replaced with fresh slag. This process was repeated 10 times, and the slag corrosion rate was subsequently measured. Samples CA-(1), CA-(3), and CA-(5) were selected in this study, along with three samples from current suppliers, to test

slag corrosion resistance. The results summarized in Table 5 ranked slag corrosion resistance from highest to lowest as follows: CA-(1) > Supplier A > CA-(3) = Supplier B > CA-(5) = Supplier C.

Due to the high-impurity content in the powder fraction of crushed spent torpedo car refractories, its addition to CA-17 tended to lower the melting point. This resulted in reduced refractoriness and consequently deteriorated resistance to molten steel penetration and slag corrosion. Furthermore, since the spent refractories used in this study consisted of high-impurity powder rather than coarse aggregate, the test was designed by removing the aggregate from CA-17 and retaining only the powder fraction (matrix area). The high-impurity spent refractories were then added to this fraction for refractoriness testing. This approach allowed direct observation of the impact of spent refractories on the refractoriness of the matrix area without interference from the aggregate region. The results shown in Table 6 indicated that refractoriness in the matrix region decreased as the proportion of spent refractory fine powders increased. Based on these results and the operational conditions of CA-17 applications, the addition of high-impurity spent refractories should be limited to 5 wt% to ensure performance stability at a maximum service temperature of 1500°C.

Table 4 Steel penetration resistance of CA-17 with different amounts of spent refractories.


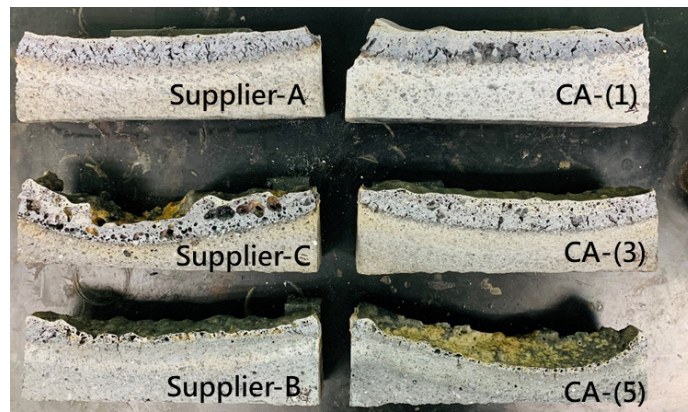
Sample	CA-(1)	CA-(2)	CA-(3)	CA-(4)	CA-(5)
Erosion Depth	14mm	15mm	16mm	18mm	21mm
Appearance					

Table 5 Slag corrosion resistance of CA-17 with different amounts of spent refractories.

Sample	CA-(1)	CA-(3)	CA-(5)	Supplier-A	Supplier-B	Supplier-C
Corrosion rate (%)	6%	23%	49%	14%	24%	51%

Appearance

**Table 6** Refractoriness of CA-17 with different amounts of spent refractories.

Refractori-ness	CA-(1)	CA-(2)	CA-(3)	CA-(4)	CA-(5)
1300°C	Pass	Pass	Pass	Pass	Pass
1400°C	Pass	Pass	Pass	Pass	Fail
1500°C	Pass	Pass	Pass	Fail	Fail
1600°C	Fail	Fail	Fail	Fail	Fail

Appearance



@1300°C

@1400°C

@1500°C

@1600°C

3.3 Phase Structure and Microstructural Observation

To further investigate the effect of varying proportions of spent refractories on the phase structure within the matrix region, high-alumina castable CA-17 was selected as the base material. The coarse aggregates of CA-17 were removed, and only the powder fraction (matrix area) was retained. The high-impurity spent refractories were then added to the matrix area. The samples were subjected to heat treatment at 1600°C for 3 hours, followed by X-ray diffraction (XRD) analysis. The results are shown in Figure 1. The analysis revealed that the phase structures of the samples containing 2.5-10 wt% spent refractories were primarily composed of corundum as the major phase. Secondary phases included $\text{CaAl}_2\text{Si}_2\text{O}_8$ (anorthite) along with minor traces of graphite and SiC. It was inferred that SiC oxidized to form SiO_x during atmospheric heat treatment. The SiO_x then reacted with Al_2O_3 in the matrix and the high-alumina cement to produce Anorthite ($\text{CaAl}_2\text{Si}_2\text{O}_8$), a triclinic structure with a melting point of 1553°C. As a result, in the XRD analysis of the matrix region, the signal intensities of the SiC and C phases originating from the spent torpedo car refractories (Al_2O_3 -SiC-C) became significantly weak. Other low-melting-point impurities, such as Fe_2O_3 , were present at very low levels and thus were not easily detected by XRD. Samples without spent refractories (CA-(1)) and with 10% addition (CA-(5)) were subjected to microstructural analysis. The results from the polarizing microscope and scanning electron microscope coupled with energy-dispersive spectroscopy (SEM/EDS) are shown in Figures 2 and 3, respectively.

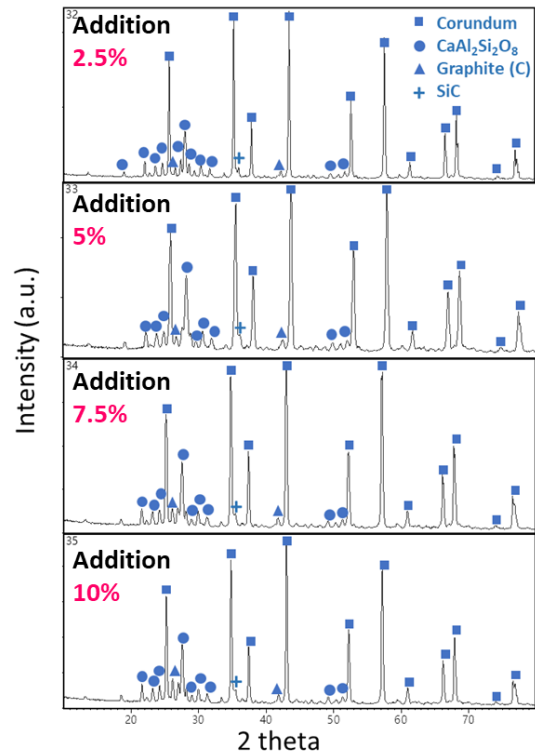


Fig.1. XRD analysis of CA-17 with different amounts of spent refractories.

From Figure 2, polarizing microscope observations, the slag/reaction layer interface of CA-(1) appeared relatively smooth. In contrast, the matrix region of CA-(5) showed more obvious erosion by slag, resulting in an uneven

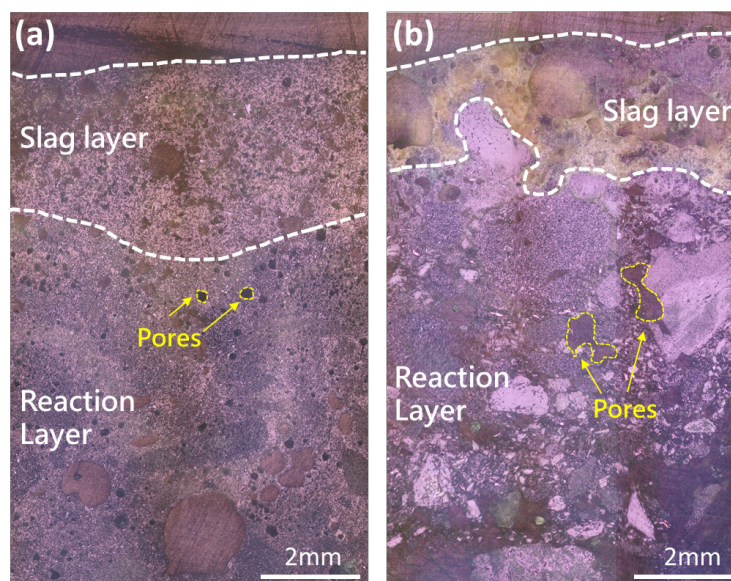


Fig.2. Polarizing microscope analysis (a) CA-(1); (b) CA-(5).

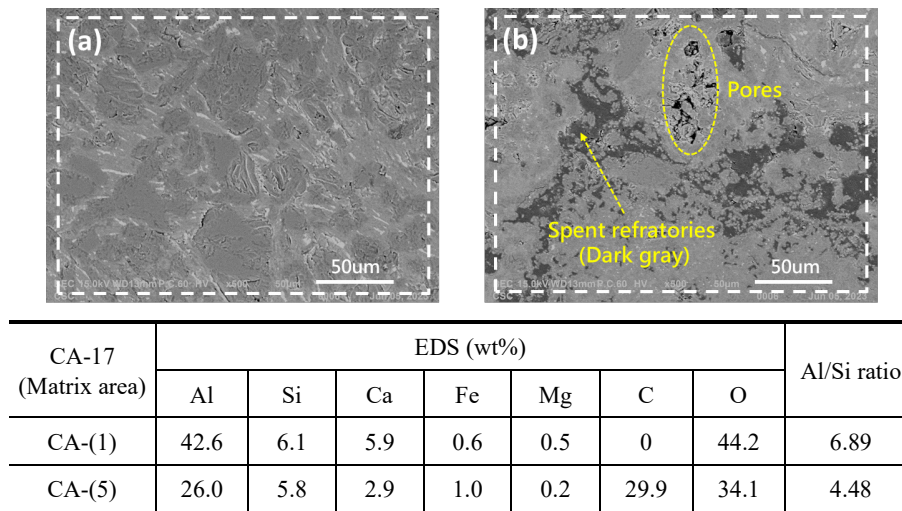


Fig.3. Scanning electron microscope SEM/EDS analysis (a) CA-(1); (b) CA-(5).

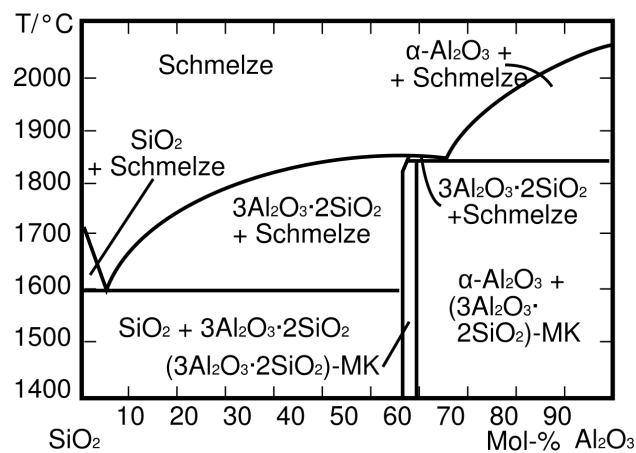


Fig.4. $\text{SiO}_2\text{-Al}_2\text{O}_3$ phase diagram⁽⁶⁾.

surface. This was attributed to the lowered melting point in the matrix region caused by the addition of high-impurity spent refractories. Furthermore, pores in CA-(1) were mostly circular, while those in CA-(5) were irregular and larger. This phenomenon was inferred to result from the carbon content in the spent refractories that reacted upon heating to produce CO_2 gas. The gas escaped and caused pore formation in the matrix. This led to strength reduction and spalling.

Figure 3 shows the SEM/EDS analysis of the matrix region. In the SEM backscattered electron (BSE) mode, the matrix of CA-(1) appeared light gray. EDS analysis identified the main elements as Al, Si, Ca, and O, corresponding to the Al_2O_3 , SiO_2 , and calcium aluminate cement in the original high-alumina castable. For the sample with 10% addition, dark gray areas corresponding to dispersed spent refractories were observed alongside the light gray matrix region. EDS spectra revealed

the presence of C signals in addition to Al, Si, Ca, and O, mainly originating from SiC and carbonaceous materials in the spent refractories. Further analysis of the Al/Si ratio in the matrix based on EDS data showed ratios of 6.89 for CA-(1) and 4.48 for CA-(5). According to the $\text{Al}_2\text{O}_3\text{-SiO}_2$ binary phase diagram (Fig.4), a lower Al/Si ratio corresponds to a lower melting point. This result aligns with the refractory performance tests. Increasing the proportion of spent refractories reduced the melting point of the CA-17 matrix and consequently lowered its refractory performance. Based on the above results, it is recommended that the maximum addition of high-impurity spent refractories not exceed 5%.

4. CONCLUSIONS

Spent torpedo car bricks are primarily recycled for use in iron-runner refractories and tap-hole clay, which utilize only the high-purity and coarse-grained fractions.

However, up to 20-30% of the spent refractory material consists of high-impurity powder with excessive levels of Fe_2O_3 and CaO , which cannot be effectively recycled. This study investigated the effects of adding high-impurity powder to high-alumina castable CA-17 at addition levels of 2.5%, 5%, 7.5%, and 10% by weight. Experimental results showed that increasing the addition of spent material slightly increased the required water content and marginally improved mechanical strength, while significantly reducing the reheating linear change. However, both apparent porosity and bulk density slightly deteriorated. These physical changes are attributed to the high levels of CaO and Fe_2O_3 in the spent, which easily react with the primary components of CA-17 (mainly Al_2O_3 and secondarily SiO_2) to form low-melting phases that promote sintering. Steel penetration tests revealed minor surface cracks without leakage across all samples, though increasing the addition of spent refractories led to greater maximum penetration depth and reduced slag corrosion resistance. Additionally, a higher addition level of spent refractories correlated with decreased refractoriness in the matrix region. Based on these results and the operational conditions of CA-17 applications, the addition of high-impurity spent refractories should be limited to 5 wt% to ensure performance stability at a maximum service temperature of 1500°C.

REFERENCES

1. Paulo H. R. Borges, Lucas F. Fonseca, Vitor A. Nunes, Tulio H. Panzera, "Andreasen Particle Packing Method on the Development of Geopolymer Concrete for Civil Engineering," *Journal of Materials in Civil Engineering*, April 2014, 26(4): 692-697.
2. Xiao-Dong Duan, En-Dong Ye, Yon-gtao Wu, "Effect of Binder on Properties of Corundum-MgO Castable," *Refractories*, 2006, 40(5): 372-375.
3. Li-Feng Dong, Pan-Long Guo, Yan-Hong Qi, "Effect of Microstructure and Composition on Castable Properties," *Baosteel Technology*, 2005, 31(5): 18-21.
4. Ben-Junl Cheng, Ping Zhang, Peng-Feil Li, Qi-Cheng Zhao, "Effect of Microsilica on Properties of Alumina-Magnesia Castable," *Bulletin of the Chinese Ceramic Society*, July 2015, 34(7): 2062-2067.
5. Li-Wan Wang, Shan-Lin Zhang, "Effect of Kyanite on the Properties of Ladle Permanent Layer Castable," *The 18th National Youth Academic Conference on Refractory Materials*.
6. [https://de.m.wikipedia.org/wiki/Datei:Phasendiagramm-SiO₂-Al₂O₃.svg](https://de.m.wikipedia.org/wiki/Datei:Phasendiagramm-SiO2-Al2O3.svg)